Trans. Phenom. Nano Micro Scales, 6(1): 49-59, Winter and Spring 2018
DOI: 10.7508/tpnms.2018.01.005

ORIGINAL RESEARCH PAPER

Optimization of 3-D natural convection around the isothermal cylinder using Taguchi method

Javad. Alinejad [1,*]***, Javad. Abolfazli Esfahani*** [2]

[1]*Department of Mechanical Engineering, Sari Branch, Islamic Azad University, Sari, Iran*
[2]*Department of Mechanical Engineering, Ferdowsi University of Mashhad, Mashhad, Iran*

Received 27 July 2016; revised 3 March 2017; accepted 10 July 2017; available online 1 January 2018

ABSTRACT: This study discusses the application of Taguchi method in assessing minimum entropy generation and maximum heat transfer rate for natural convection in an enclosure embedded with isothermal cylinder. The simulations were planned based on Taguchi's L25 orthogonal array with each trial performed under different conditions of position and aspect ratio (AR) of the cylinder. The thermal lattice Boltzmann based on D3Q19 methods without any turbulent submodels was purposed to simulate the flow and thermal fields. A relaxation time method with the stability constants is introduced to solve turbulent natural convection problems. Signal-to-noise ratios (S/N) analysis were carried out in order to determine the effects of process parameters and optimal factor settings. Finally, confirmation tests verified that Taguchi method achieved optimization of heat transfer rate with sufficient accuracy.

KEYWORDS: *Cylinder; Lattice Boltzmann model; Natural convection; Taguchi method*

INTRODUCTION

The main idea of this study is simulation of natural convection in a cavity with a heat source. This simulation is more important in industrial and technological applications including, electronic cooling [1], cooling of the reactors [2, 3], heat and mass transfer processes in cryogenic fuel and vertical storage tanks [4−9]. In these works, the regimes of convective heat transfer in closed vertical volumes were analyzed in detail for the conditions when the thermal fluxes supplied to the liquid are uniformly distributed over the bottom and lateral surfaces. The spatial and temporal structure of convection at a sine distribution of the thermal flux on the lateral wall of the vertical cylinder was presented in [10]. The mathematical modeling of unsteady regimes of natural convection in a closed cylindrical region with a heat-conducting shell of finite thickness was carried out in [11]. Numerous studies of various convective flow based on entropy generation minimization (EGM) are reported in literature [12–15]. Chatterjee and Chakraborty [12] examined the numerical formulation involving second law of thermodynamics for entropy generation analysis of three-dimensional surface tension driven turbulent transport during laser materials processing. Esfahani and Alinejad [13] analyze the entropy generation due to conjugate natural convection in an enclosure. Transition criteria for entropy reduction of convective heat transfer from micropatterned surfaces were reported by Naterer [14].

*Corresponding Author Email: *Alinejad_javad@iausari.ac.ir*
Tel.: +989121083680; Note. This manuscript was submitted on *July* 27, 2016; approved on *March* 3, 2017; published online *January 1, 2018*

Entropy generation in microchannel flow with presence of nanosized phase change particles was investigated by Alquaity et al. [15]. Recently Lattice Boltzmann Method (LBM) has been developed as a new tool for simulating the fluid flow, heat transfer and other complicated physical phenomena. Compared with the traditional computational fluid dynamics methods, the Lattice Boltzmann Method is a meso-scale modeling method based on the particle kinematics. It has many advantages, such as simple coding, easy implementation of boundary conditions and fully parallelism. At present the applications of LBM have achieved great success in multi-phase flow, chemical reaction flow, thermal hydrodynamics, suspension particle flow and magneto hydrodynamics. Esfahani and Alinejad [16] conducted the simulation for viscous-fluid flow and conjugate heat transfer in a rectangular cavity by using LBM. D'Orazio et al. [17] performed the numerical calculations for the natural convection in a cavity. In the different study several designs of experiments (DOE) approaches have been applied to improve the efficiency of thermal system. A number of research studies have reported that the Taguchi design is an ideal method. The Taguchi approach is a simple and easy tool, which provides effective solutions on a design, as it emphasizes a mean performance value close to the target value. In this way, significant factors that have a significant impact on the experimental condition could be recognized and the optimal performance is determined [18-20]. This Paper investigates the natural convection heat transfer in a three-dimensional cavity with the presence of an isothermal cylinder as a heat

Nomenclature

		Greek Symbols	
g	Gravitational acceleration, ms^{-2}	α	Thermal diffusivity, m^2s^{-1}
T	Temperature, K	υ	kinematic viscosity, m^2s^{-1}
u, v, w	Velocities, ms^{-1}	θ	Dimensionless temperature
x, y, z	Coordinates, m		**Subscripts**
Nu_l	Local Nusselt number	c	cold
Nu_m	Mean Nusselt number	f	fluid
Pr	Prandtl number, (υ/α)	h	hot
Ra	Rayleigh number, $(g\beta\Delta TH^3)/(\alpha\upsilon)$	s	solid
Re	Reynolds number, $(R\omega)H/(\upsilon)$		

source by means of Taguchi method in order to obtain significant process parameters and optimum factor combinations. For this reason the thermal Lattice-Boltzmann method with the Boussinesq approximation is employed to simulate natural convection. The effects of cylinder aspect ratio and position has been observed and analyzed in detail. The present results provide a good approximation for choosing effective parameters of designing thermal system.

LATTICE BOLTZMANN METHOD

The lattice Boltzmann method is particularly successful as a numerical method for solving the different fluid dynamic problems [21-23]. LBM is derived from lattice gas methods as an explicit discretization of the Boltzmann equation in the phase space is considered. LBM is a vigorous numerical method, based on the kinetic theory to simulate fluid flow and heat transfer [24-25]. Unlike the classical macroscopic approach (Navier- Stokes) the lattice Boltzmann is a mesoscopic model to simulate flow field [25-26]. In this approach, the fluid domain is made discrete in uniform Cartesian cells, each one of which holds a fixed number of distribution functions (DF) that represent the number of fluid particles moving in these discrete directions. Hence depending on the dimension and number of velocity directions, there are different models that can be used. The present study examined three-dimensional flow by using 3-D lattice with nineteen velocities (D3Q19 model). The velocities of the D3Q19 model are shown in Figure. 1. The LB Model used in the present work is the same as that employed in [27- 29]. The DFs are calculated by solving the Lattice Boltzmann Equation (LBE), which is a special discretization of the kinetic Boltzmann equation. After introducing Bhatnagar–Gross–Krook (BGK) approximation, the Boltzmann equation can be formulated as below [22]:

$$f_k(x+c_k\Delta t, t+\Delta t) = f_k(x,t) + \frac{\Delta t}{\tau}\left[f_k^{eq}(x,t) - f_k(x,t)\right] + \Delta t c_k F_k \quad (1)$$

Where Δt, c_k, τ, f_k^{eq}, F_k denote lattice time step, the discrete lattice velocity in direction k, the lattice relaxation time, the equilibrium DF, and the external force in the direction of the lattice velocity, respectively.

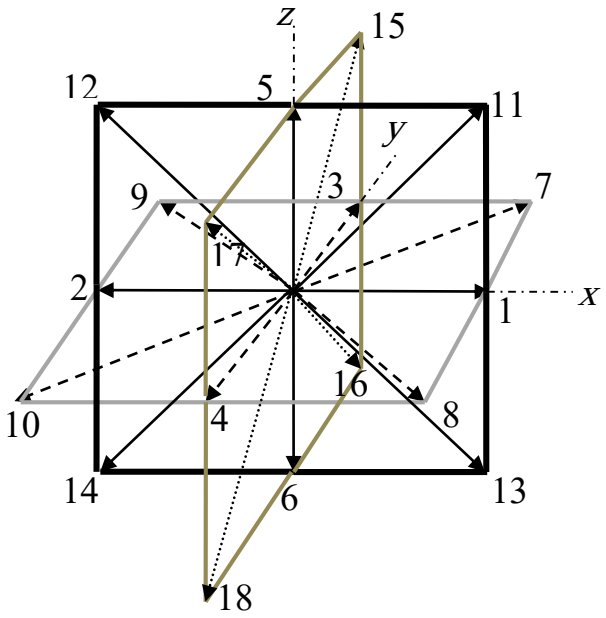


Fig. 1. 3-D with 19-velocities lattice (D3Q19) model

The equilibrium distribution function for the D3Q19 velocity model is given by

$$f_k^{eq}(x,t) = \omega_k \rho^{\sigma}\left[1 + \frac{3c_k \cdot u}{c^2} + \frac{9(c_k \cdot u)^2}{2c^2} - \frac{3u^2}{2c^2}\right] \quad (2)$$

where $\omega_0 = \frac{1}{3}$, $\omega_k = \frac{1}{18}$ for k=1-6 and $\omega_k = \frac{1}{36}$ for k=7-18. In order to incorporate buoyancy force in the model, the force term in equation 1 needs to be calculated, as below, in a vertical direction (z):

$$F = \rho g_z \beta \Delta T \quad (3)$$

The macroscopic fluid densities and velocities are computed as below:

$$\rho = \sum_{k=0}^{18} f_k, \quad u = \frac{1}{\rho}\sum_{k=0}^{18} f_k c_k \quad (4)$$

For the temperature field the g distribution is as below:

$$g_k(x + c_k\Delta t, t + \Delta t) = g_k(x,t) + \frac{\Delta t}{\tau_g}\left[g_k^{eq}(x,t) - g_k(x,t)\right] \quad (5)$$

For the D3Q19 model, the equilibrium energy distribution functions can be defined as follows:

$$g_0^{eq} = -\frac{T}{2}\frac{u^2}{c^2} \quad (6)$$

$$g_{1-6}^{eq} = \frac{T}{18}\left[1 + \frac{c_k \cdot u}{c^2} + \frac{9(c_k \cdot u)^2}{2c^2} - \frac{3u^2}{2c^2}\right] \quad (7)$$

$$g_{7-18}^{eq} = \frac{T}{36}\left[2 + 4\frac{c_k \cdot u}{c^2} + \frac{9(c_k \cdot u)^2}{2c^4} - \frac{3u^2}{2c^2}\right] \quad (8)$$

The temperature field is computed as:

$$T = \sum_{k=0}^{18} g_k \quad (9)$$

Natural convection stability constant (sc)

For stable and convergence solution in natural convection the maximum velocity should not exceed the critical magnitude ($u_{max} \leq 0.1$) in terms of compressibility effect and the relaxation time must be as large as possible. For these reasons we use the scale analysis of the natural convection boundary layer to find the suitable relaxation time as follows:

$$For\ Pr < 1:\ u_{max} \sim \frac{\vartheta}{H}\left(\frac{Ra}{Pr}\right)^{1/2};\quad Ma = \frac{u_{max}}{c_s} \quad (10)$$

$$For\ Pr > 1:\ u_{max} \sim \frac{\vartheta}{H}\left(\frac{Ra^{1/2}}{Pr}\right);\quad Ma = \frac{u_{max}}{c_s} \quad (11)$$

Proportionalities (10) and (11) can be converted to equalities using constants sc1 and sc2. These constants could be calculated for different geometries by solving the problem in a more stable condition.

For instance, by comparing the two sides of these inequalities, we obtained sc1 = 0.25 for a 2-D convective square cavity problem with Ra = 106.

The fact that sc1, and sc2, is less than unity is an important result, which has not been mentioned in the previous works. The significance of this point would be discovered later on.

$$For\ Pr < 1: u_{max} = sc_1\frac{\vartheta}{H}\left(\frac{Ra}{Pr}\right)^{1/2} \quad (12)$$

$$For\ Pr > 1: u_{max} = sc_2\frac{\vartheta}{H}\left(\frac{Ra^{1/2}}{Pr}\right) \quad (13)$$

Substituting $u_{max} \leq 0.1$ and solving for ϑ:

$$For\ Pr < 1: \vartheta \leq \frac{0.1}{sc_1}\left(\frac{Pr}{Ra}\right)^{1/2} H \quad (14)$$

$$For\ Pr > 1: \vartheta \leq \frac{0.1}{sc_2}\left(\frac{Pr}{Ra^{1/2}}\right) H \quad (15)$$

By these equations the relaxation times calculated as below:

$$Pr < 1 \begin{cases} \tau \leq \left(\frac{0.1}{sc_1}\right)\left(\frac{1}{c_s^2\,\Delta t}\right)\left(\frac{Pr}{Ra}\right)^{1/2} H + 0.5 & (16) \\ \tau_g \leq \left(\frac{0.1}{sc_1}\right)\left(\frac{1}{c_s^2\,\Delta t}\right)\left(\frac{1}{RaPr}\right)^{1/2} H + 0.5 & (17) \end{cases}$$

$$Pr > 1 \begin{cases} \tau \leq \left(\frac{0.1}{sc_2}\right)\left(\frac{1}{c_s^2\Delta t}\right)\left(\frac{Pr}{Ra^{1/2}}\right) H + 0.5 & (18) \\ \tau_g \leq \left(\frac{0.1}{sc_2}\right)\left(\frac{1}{c_s^2\Delta t}\right)\left(\frac{1}{Ra^{1/2}}\right) H + 0.5 & (19) \end{cases}$$

Nusselt number

Heat transfer between hot and cold walls was computed by local and mean Nusselt number which is given as

$$Nu_l = \frac{-1}{\theta_m}\frac{\partial\theta}{\partial n}\Big|_{wall} \quad , \quad \theta_m = \frac{T - T_C}{T_h - T_C} \quad (20)$$

$$Nu_m = \frac{1}{l}\int_0^l Nu_l\, dx \quad (21)$$

Entropy generation

$$N_s = \left[\left(\frac{\partial\theta}{\partial x}\right)^2 + \left(\frac{\partial\theta}{\partial y}\right)^2\right] + \phi\left[2\left(\frac{\partial u}{\partial x}\right)^2 + 2\left(\frac{\partial v}{\partial y}\right)^2 + \left(\frac{\partial u}{\partial y} + \frac{\partial v}{\partial x}\right)^2\right]; \quad \phi = \frac{\mu T_0}{k}\left(\frac{\alpha}{H\Delta T}\right)^2 \quad (22)$$

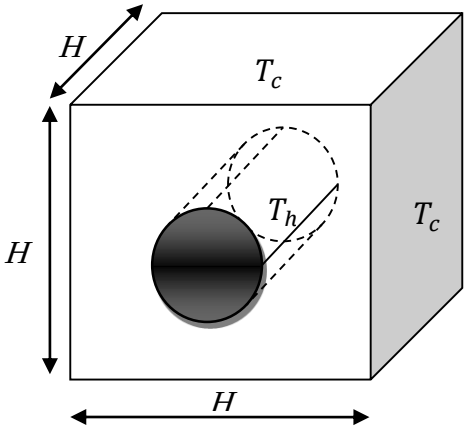
$$S_g = \int_{\forall} N_s\, d\forall \quad (23)$$

PHYSICAL MODEL

The physical geometry considered in this study is shown in Figure 2. We consider the natural convection of a viscous incompressible fluid in a three dimensional enclosure in the presence of a solid local energy source with constant temperature T_h and the wall temperature of the cavity are

constant which contact to the outside with the ambient temperature (T_c).

When doing numerical simulation it was assumed that the thermophysical properties of the material are temperature-independent. In the present study the flow is bounded by an enclosure with the geometric setup, where $D = 2\sqrt{ab}$ and $H = 5D$ denote the cylinder diameter and the height of the cavity, respectively.



Aspect Ratio: AR=*a/b*

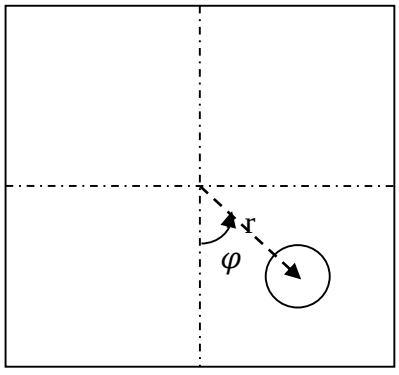


Fig. 2. Schematic diagrams of the cavity and different cylinders

Curved boundary treatment

Figure 3a shows the imaginary part of the curved boundary, where the black small circles (x_w), the open circles (x_f) and the grey circles (x_b) represent the boundary, the fluid region and the solid region nodes, respectively. To apply the boundary conditions and completion of the streaming step, the reflected distribution function $\tilde{f}(x_b, t)$ on the curved boundary must be calculated. The Distance between the boundary and the fluid nodes as a fraction of the total distance between solid and fluid nodes is calculated as follows:

$$\Delta = \frac{\|x_f - x_w\|}{\|x_f - x_b\|} \tag{24}$$

Figures 3(b-d) show the three type of the possible boundary between the solid and fluid nodes. In all these conditions the reflected distribution function are unknown, which must be calculated.

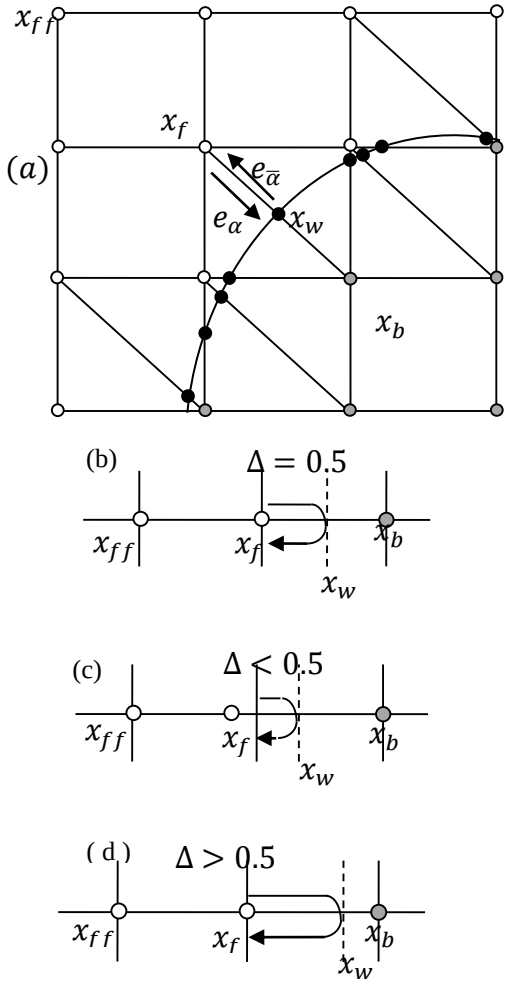


Fig. 3. Layout of the regularly spaced lattices and curved wall boundary, (a) overall view. (b) $\Delta = 0.5$,(c) $\Delta < 0.5$, (d) $\Delta > 0.5$

This method is pointed in [30]. The post-collision distribution function is conducted as

$$\begin{aligned}\tilde{f}_{\bar{\alpha}}(x_b, t + \Delta t) = {} & (1-\lambda)\tilde{f}_{\alpha}(x_f, t + \Delta t) \\ & + \lambda f_{\alpha}^{0}(x_b, t + \Delta t) \\ & - 2\frac{3}{c^2}\omega_\alpha \rho(x_f, t + \Delta t) e_\alpha \cdot u_w\end{aligned} \tag{25}$$

Where

$$f_\alpha^0(x_b, t+\Delta t) = f_\alpha^{eq}(x_f, t+\Delta t) + \frac{3}{c^2} w_\alpha \rho(x_f, t+\Delta t) e_\alpha (u_{bf} - u_f) \quad (26)$$

$$u_{bf} = u_{ff}, \lambda = \frac{2\Delta - 1}{\tau_m - 2} \quad if \quad 0 < \Delta \leq \frac{1}{2} \quad (27a)$$

$$u_{bf} = \left(1 - \frac{3}{2\Delta}\right) u_{f+} \frac{3}{2\Delta} u_w, \quad \lambda = \frac{2\Delta - 1}{\tau_m + \frac{1}{2}} \quad if \quad \frac{1}{2} < \Delta \leq 1 \quad (27b)$$

Grid independency

For grid independency, the average Nusselt number was calculated at high Ra numbers for different grid points.

As seen in table 1 for grid points passing from 80×80×80 to 100×100×100 for Ra = 106 and from 150×150×150 to 200×200×200 for 109 , respectively, no considerably change in the average Nusselt number is observed (maximum variation is less than 0.3 %). According to the Table 1, the 100×100×100 grid points was used for Ra ≤ 108 and 200×200×200 grid points was used only for Ra = 109.

Table 1
Effect of spatial resolution on the mean Nusselt number at different Rayleigh numbers.

Mesh size	40 ×40 ×40	80 ×80 ×80	100 ×100 ×100	150 ×150 ×150	200 ×200 ×200
Ra= 10^6	8.815	8.843	8.845	-	-
Ra= 10^9	-	-	52.374	53.116	53.264

CODE VALIDATION

The numerical simulation was done by an in-house code written in FORTRAN, using LBM. Numerical investigations were carried out for the following values of dimensionless Rayleigh number, 10^3<Ra<10^9. The influence of the main parameters characterizing the process was analyzed.

The obtained results are compared with the previous 2-D and 3-D simulations of natural convection in a square cavity [33-38].

The comparison of streamlines, isotherms and mean Nusselt number at the interface between the solid wall and gaseous cavity with previous work at different Rayleigh numbers illustrates a fine agreement that has been obtained (figure 4 and table 2).

The isotherm lines vortex indicates a change in the dominant heat transfer mechanism with Rayleigh number. For low Rayleigh number, isotherms are aligned with the temperature constant walls and slightly deviated by the flow, and the heat is transferred mainly by heat conduction. As Ra increases, the controlling heat transfer mechanism changes from conduction to convection, the shape of isotherms begins to bend in the bulk region. The isotherm lines become flat in the central region of the cavity. These lines are vertical only in thin boundary layers near the hot and cold walls and the fluid is thermally arranged in different layers.

In other words, the isotherms become horizontal in the cavity.

Observing the streamlines patterns reveals wavy disturbances occurrence close to the horizontal adiabatic boundary specially at upper-left and bottom right corners. These patterns intensify by increasing Ra to10^8 and finally eddies are developed.

The temperature field becomes more and more stratified. The isotherms near the hot wall stretch upward as a result of the warm fluid wake.

Finally, It should be noted that there is an excellent agreement between the present results and the benchmark LBM 2-D solution by Du et al. [31] and Dixit et al. [32] and 3-D solution by Peng et al. [34] for all values of Ra (maximum difference is less than 8%), as well as with the CFD 2-D solutions by Barakos et al. [33] and 3-D solutions by Bocu and Altac [35] (maximum difference is less than 4%).

Table 2
Comparison of our results at mid-plane (x=0.5) with the bench-mark data.

Ra	10^3	10^4	10^5	10^6	10^7	10^8	10^9
Our results	1.113	2.231	4.520	8.845	16.499	29.590	53.264
Ref. [17]	1.117	2.235	4.504	8.767	-	-	-
Ref. [31]	1.108	2.252	4.596	8.822	16.424	29.094	49.110
Ref. [32]	1.121	2.286	4.546	8.652	16.790	30.506	57.350
Ref. [33]	1.114	2.245	4.510	8.806	-	30.1	54.4
Ref. [34]	1.099	2.304	4.658	-	-	-	-
Ref. [35]	1.070	2.057	4.359	8.794	17.267	-	-

Figure 5 shows the variations of dimensionless temperature and the vertical velocity profiles, along the mid-height line of cavity for different Rayleigh number. It can be seen that, by increasing the Ra number these profiles begin to bend near the vertical hot and cold walls. Also, it can be found that very close to the hot wall, the temperature profiles are nearly linear and near the cold wall are almost anti-symmetric.

It can be seen that, there is a good agreement between the present prediction and the previous data.

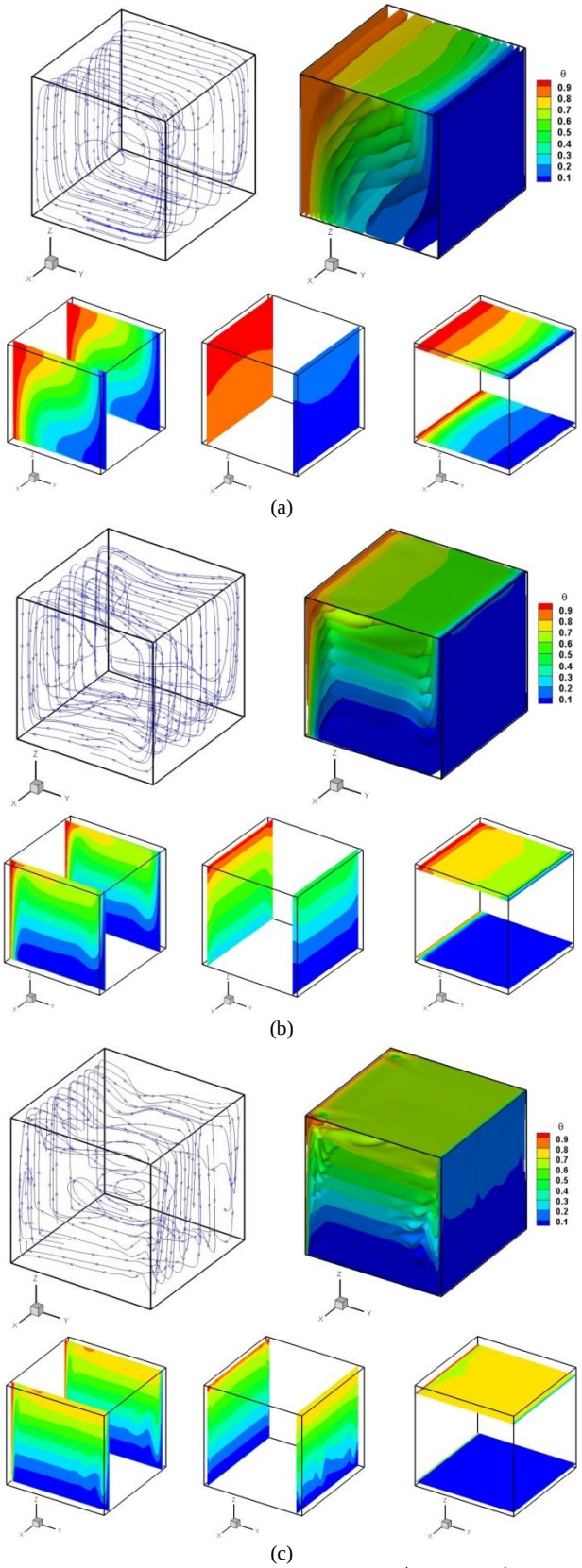


Fig. 4. Streamlines and Isotherms at (a) Ra=10^4, (b) Ra=10^6, (c) Ra=10^8

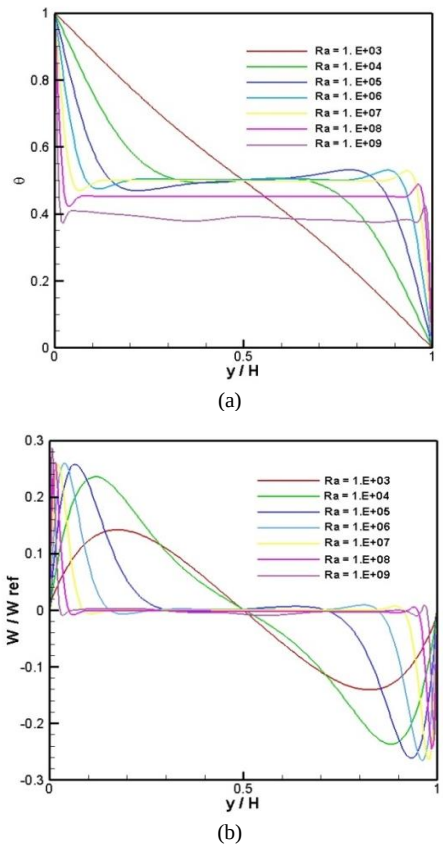


Fig. 5. Temperature profile (a) and velocity profile (b) for different Rayleigh number at x/H=0.5

RESULTS AND DISCUSSION

The effect of different aspect ratio

The streamlines (figure 6a) and isotherms (figure 6b) are observed in Figure 6.

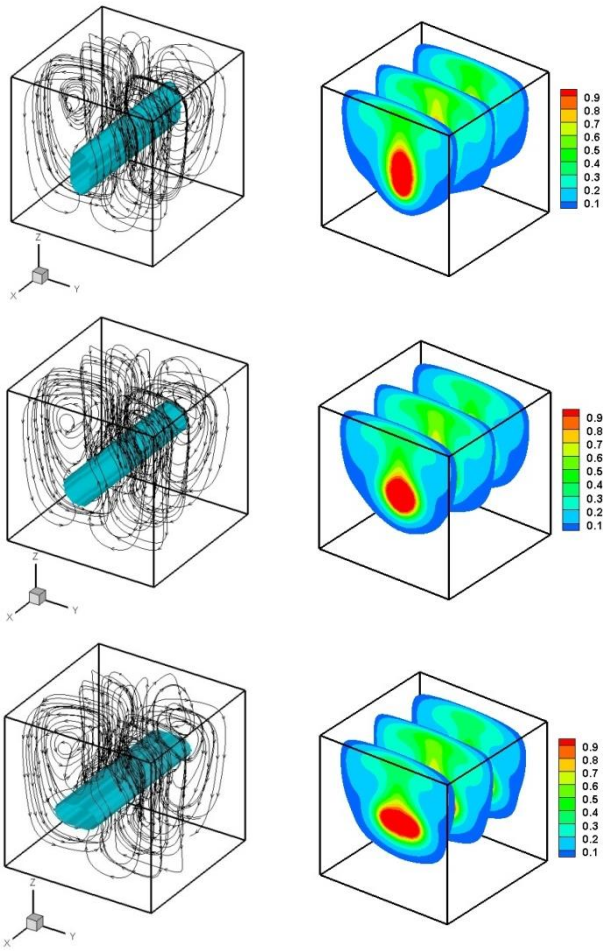
Illustrative figures are shown at Ra=10^5 and different AR (Aspect Ratio, AR=a/b) in various cases.

As a result of the buoyancy effect, the fluid from the heat source in the cavity rises and flow down along the vertical walls forming two main rolls in the cavity. A detailed examination of the streamlines and isotherms clearly shows that the cold fluid is entrained towards the heated cylinder which, in turn, rises upward there by setting up a buoyancy induced flow which transports heat from the heated cylinder to the cold ambient.

In addition, this phenomenon gives rise to the formation of two main circulations.

The main circular cells occupy a region between left and right vertical wall. The effect of the shape of the cylinder cross section (aspect ratio AR=a/b) is also seen to be significant.

For instance, in the case of the so-called slender configuration (AR <1), the plume was seen to be smaller than that for a circular cylinder (AR=1) otherwise under identical conditions. Of course, the reverse trend is seen for blunt configuration (AR>1).



(a) (b)

Fig. 6. Streamlines (a) and isotherms (b) for cylinders with different cross section, Ra=10^5

Application of the Taguchi method

Taguchi method is proposed by Taguchi in 1960s. This method is widely applied for improving industrial product quality greatly [36-37]. In addition to this, low trial numbers, obtaining the effects of process parameters on quality characteristics and their optimum levels has easily increased its popularity.

In the present study, the effects of aspect ratio and position of the cylinder on heat transfer rate (Nu) and entropy generation (Sg) have been determined and optimum factor levels have been obtained by analyzing Taguchi method.

The number of simulation can be reduced by means of Taguchi technique, Based on orthogonal arrays. This method uses the special design of orthogonal arrays to learn the whole parameters space with small number of experiments.

In the present study, an L25 orthogonal array by three factors with five levels is chosen as shown in Table 3. To get more accurate in terms of the heat transfer rate, the Nusselt numbers over the wall of the cavity and entropy generation number in flow field for various designated trial have been calculated.

Taguchi method employs a signal-to-noise ratio (S/N) to measure the present variation.

Also, in calculation procedure the effect of different control factors and their interaction was assumed. In Taguchi designs, a measure of robustness used to identify control factors that reduce variability in a product or process by minimizing the effects of uncontrollable factors (noise factors).

Higher values of the signal-to-noise ratio (S/N) identify control factor setting that minimize the effects of the noise factors.

The definition of S/N ratio differs according to an objective function, i.e., a characteristic value.

There are three kinds of characteristic value: Nominal is Best (NB: n = 10 Log10 [square of mean/variance]), Smaller is Better (SB: n = -10 Log10 [mean of sum of squares of measured data]) and Larger is Better (LB: n = -10 Log10 [mean of sum squares of reciprocal of measured data]). As the minimum entropy generation (Sg) is the one of the major goal in present study, SB is chosen as a characteristic value. S/N ratios plots for different factors are given in Figure 7.

As a result, the optimum settings of control factors minimizing the entropy generation are AR=2, r=0.7 R and φ=135o.

Table 3
L25 Orthogonal array with control factors.

Aspect Ratio		Radius (r)	Angle (φ)	Sg	Nu
AR = $^1/_2$		0	0º	280	1.906
		0.3 R	45º	339	1.807
		0.5 R	90º	211	1.751
		0.6 R	135º	73	1.929
		0.7 R	180º	84	2.884
AR = $^2/_3$		0	45º	273	1.858
		0.3 R	90º	255	1.793
		0.5 R	135º	93	1.645
		0.6 R	180º	99	1.839
		0.7 R	0º	349	1.442
AR = 1		0	90º	262	1.788
		0.3 R	135º	158	1.630
		0.5 R	180º	112	1.629
		0.6 R	0º	354	1.524
		0.7 R	45º	136	1.665
AR = $^3/_2$		0	135º	256	1.756
		0.3 R	180º	162	1.635
		0.5 R	0º	353	1.604
		0.6 R	45º	220	1.544
		0.7 R	90º	150	2.370
AR = 2		0	180º	254	1.748
		0.3 R	0º	329	1.721
		0.5 R	45º	241	1.531
		0.6 R	90º	167	1.911
		0.7 R	135º	40	3.005

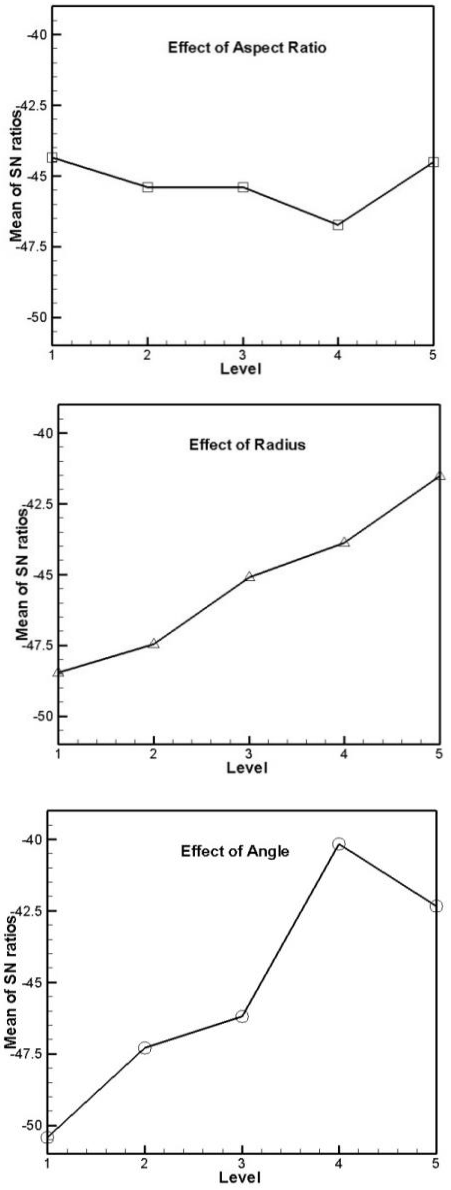


Fig. 7. S/N ratios plots for minimum entropy generation

The second objective function is the maximum heat transfer rate (Nu), so LB is chosen as a characteristic value. S/N ratios plots for different factors are given in Figure 8. As a result, the optimum settings of control factors maximizing the Nusselt number are AR=1/2, r=0.7 R and φ=135o.

Finally the combination of the maximum heat transfer rate and minimum entropy generation is chosen as a major objective function. S/N ratios plots for different factors are given in Figure 9.

As a result, the optimum settings of control factors maximizing the Nusselt number and minimizing the entropy generation are AR=1/2, r=0.7 R and φ=135o. The final step in verifying results based on Taguchi design is the confirmation test.

Figure 10 shows the streamlines and isotherms for optimal factor settings. Numerical results indicate that the Nusselt number and entropy generation in this case are equal to 3.057 and 54, respectively.

It can be concluded that Taguchi method achieves the Statistical assessment of maximum heat transfer rate and minimum entropy generation of natural convection in an enclosure embedded with isothermal cylinder.

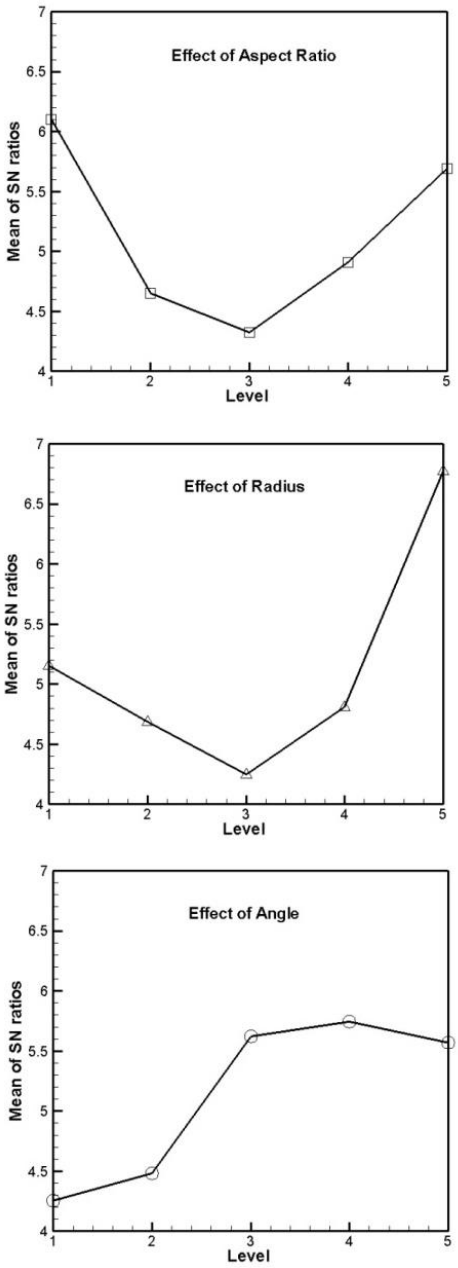


Fig. 8. S/N ratios plots for maximum heat transfer rate

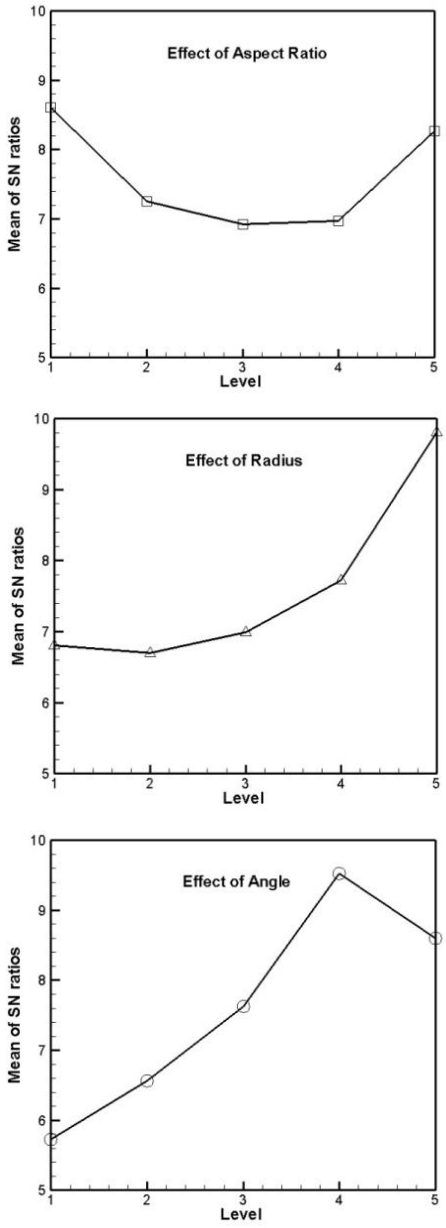
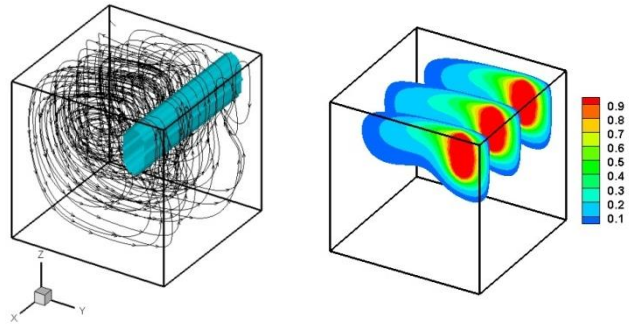


Fig. 9. S/N ratios plots for the combination of the maximum heat transfer rate and minimum entropy generation



(a) (b)

Fig. 10. Streamlines (a) and isotherms (b) for cylinders with different cross section, Ra=105

CONCLUSION

In this article, effect and optimization of different parameters in natural convection in a three-dimensional cavity with the presence of a hot cylinder on maximum Nusselt number and minimum entropy generation were investigated through Taguchi method. The practical benefit of this study is that the use of obtained optimum condition increases the heat transfer rate and decreases the entropy generation. The simulation is numerically predicted by using Lattice Boltzmann Method. In conclusion, some of the main points are briefly remarked:

- In comparison with complicated model such as large-eddy simulation or MRT, using the mentioned technique to simulate turbulent natural convection in the present study having a simple calculation procedure.
- Comparisons of the results with previous work at high Rayleigh numbers show that a very good agreement has been obtained.
- Based on the SN ratio plots, all control factors have significant effect on the quality characteristic statistically.
- The optimum condition with the maximum Nusselt number was obtained on the fourth level of radius (r=0.7 R), the third level of angle (φ =135o) and the first level of aspect ratio (AR=1/2).
- The optimum condition with the minimum entropy generation was obtained on the fourth level of radius (r=0.7 R), the third level of angle (φ =135o) and the fifth level of aspect ratio (AR=2).
- The optimum condition with the combination of the maximum heat transfer rate and minimum entropy generation was obtained on the fourth level of radius (r=0.7 R), the third level of angle (φ =135o) and the first level of aspect ratio (AR=1/2).
- The confirmation test including optimum condition was conducted and the obtained result indicates that Taguchi method can be used in the optimization of mix convection cooling successfully.

REFERENCES

[1] Samadiani E, Joshi Y, Mistree F. The thermal design of a next generation data center: a conceptual exposition. Journal of Electronic Packaging. 2008 Dec 1;130(4):041104.

[2] Kim YK, Lee KH, Kim HR. Cold neutron source at KAERI, Korea. Nuclear Engineering and Design. 2008 Jul 31;238(7):1664-9.

[3] Karthikeyan S, Sundararajan T, Shet US, Selvaraj P. Effect of turbulent natural convection on sodium pool combustion in the steam generator building of a fast breeder reactor. Nuclear Engineering and Design. 2009 Dec 31;239(12):2992-3002.

[4] Rodriguez I, Castro J, Pérez-Segarra CD, Oliva A. Unsteady numerical simulation of the cooling process of vertical storage tanks under laminar natural convection. International Journal of Thermal Sciences. 2009 Apr 1;48(4):708-21.

[5] Lin W, Armfield SW. Direct simulation of natural convection cooling in a vertical circular cylinder. International Journal of Heat and Mass Transfer. 1999 Nov 30;42(22):4117-30.

[6] Kurian V, Varma MN, Kannan A. Numerical studies on laminar natural convection inside inclined cylinders of unity aspect ratio. International Journal of Heat and Mass Transfer. 2009 Jan 31;52(3):822-38.

[7] Cherkasov SG. Natural convection and temperature stratification in a cryogenic fuel tank in microgravity. Fluid dynamics. 1994 Sep 1;29(5):710-6.

[8] Polezhaev VI, Cherkasov SG. Unsteady thermal convection in a cylindrical vessel heated from the side. Fluid Dynamics. 1983 Jul 1;18(4):620-9.

[9] Cherkasov SG. Natural convection in a vertical cylindrical vessel with heat supplied to its side and free surfaces. Fluid Dynamics. 1984 Nov 1;19(6):902-6.

[10] Moiseeva LA,Cherkasov SG.Mathematical modeling of natural convection in a vertical cylindrical tank with alternating-sign heat flux distribution on the wall. Fluid dynamics. 1996 Mar 1;31(2):218-23.

[11] Sheremet MA.Unsteady conjugate thermogravitation-al convection in a cylindrical region with local energy source. Thermophysics and Aeromechanics. 2011 Sep 1;18(3):447-58.

[12] Chatterjee D, Chakraborty S. Entropy generation analysis of turbulent transport in laser surface alloying process. Materials science and technology. 2006 Jun 1;22(6):627-33.

[13] Esfahani JA, Alinejad J. Entropy generation of conjugate natural convection in enclusures: the lattice Boltzmann method. Journal of Thermophysics and Heat Transfer. 2013 Jul 16.

[14] Naterer GF. Transition criteria for entropy reduction of convective heat transfer from micropatterned surfaces. Journal of Thermophysics and Heat Transfer. 2008 Apr 1;22(2):271-80.

[15] Alquaity AB, Al-Dini SA, Yilbas BS. Entropy generation rate in microchannel flow with phase change particles. Journal of Thermophysics and Heat Transfer. 2012 Jan 1;26(1):134-40.

[16] Esfahani JA,Alinejad J.Lattice Boltzmann simulation of viscous-fluid flow and conjugate heat transfer in a rectangular cavity with a heated moving wall. Thermophysics and Aeromechanics. 2013 Oct 1;20(5):613-20.

[17] D'Orazio A, Corcione M, Celata GP. Application to natural convection enclosed flows of a lattice Boltzmann BGK model coupled with a general purpose thermal boundary condition. International Journal of Thermal Sciences. 2004 Jun 1;43(6):575-86.

[18] Xie J,Yuan C. Parametric study of ice thermal storage system with thin layer ring by Taguchi method. Applied Thermal Engineering. 2016 Apr 5;98:246-55.

[19] Do Kim K,Choi DW,Choa YH,Kim HT.Optimization of parameters for the synthesis of zinc oxide nanoparticles by Taguchi robust design method. Colloids and Surfaces A: Physicochemical and Engineering Aspects. 2007 Dec 1;311(1):170-3.

[20] Huang CN, Yu CC. Integration of Taguchi's method and multiple-input, multiple-output ANFIS inverse model for the optimal design of a water-cooled condenser. Applied Thermal Engineering. 2016 Apr 5;98:605-9.

[21] Chopard B,Luthi PO.Lattice Boltzmann computations and applications to physics. Theoretical Computer Science. 1999 Mar 28;217(1):115-30.

[22] Nourgaliev RR, Dinh TN, Theofanous TG, Joseph D. The lattice Boltzmann equation method: theoretical interpretation, numerics and implications. International Journal of Multiphase Flow. 2003 Jan 31;29(1):117-69.

[23] Yu D, Mei R, Luo LS, Shyy W. Viscous flow computations with the method of lattice Boltzmann equation. Progress in Aerospace Sciences. 2003 Jul 31;39(5):329-67.

[24] Mohamad AA. Applied lattice Boltzmann method for transport phenomena, momentum, heat and mass transfer. Canadian Journal of Chemical Engineering. 2007 Dec 1;85(6):946-.

[25] Delavar MA, Farhadi M, Sedighi K. Effect of the heater location on heat transfer and entropy generation in the cavity using the lattice Boltzmann method. Heat Transfer Research. 2009;40(6).

[26] Mezrhab A, Jami M, Abid C,Bouzidi MH, Lallemand P. Lattice-Boltzmann modelling of natural convection in an inclined square enclosure with partitions attached to its cold wall. International journal of heat and fluid flow. 2006 Jun 30;27(3):456-65.

[27] He X, Luo LS. Lattice Boltzmann model for the incompressible Navier–Stokes equation. Journal of statistical Physics. 1997 Aug 1;88(3):927-44.

[28] Kao PH, Yang RJ. Simulating oscillatory flows in Rayleigh–Benard convection using the lattice Boltzmann method. International Journal of Heat and Mass Transfer. 2007 Aug 31;50(17):3315-28.

[29] Wang J, Wang D, Lallemand P, Luo LS. Lattice Boltzmann simulations of thermal convective flows in two dimensions. Computers & Mathematics with Applications. 2013 Jan 31;65(2):262-86.

[30] Du R, Liu W. A new multiple-relaxation-time lattice Boltzmann method for natural convection. Journal of Scientific Computing. 2013 Jul 1;56(1):122-30.

[31] Du R, Liu W. A new multiple-relaxation-time lattice Boltzmann method for natural convection. Journal of Scientific Computing. 2013 Jul 1;56(1):122-30.

[32] Dixit HN, Babu V. Simulation of high Rayleigh number natural convection in a square cavity using the lattice Boltzmann method. International journal of heat and mass transfer. 2006 Feb 28;49(3):727-39.

[33] Barakos G, Mitsoulis E, Assimacopoulos D. Natural convection flow in a square cavity revisited: laminar and turbulent models with wall functions. International Journal for Numerical Methods in Fluids. 1994 Apr 15;18(7):695-719.

[34] Peng Y, Shu C, Chew YT. A 3D incompressible thermal lattice Boltzmann model and its application to simulate natural convection in a cubic cavity. Journal of Computational Physics. 2004 Jan 1;193(1):260-74.

[35] Bocu Z, Altac Z. Laminar natural convection heat transfer and air flow in three-dimensional rectangular enclosures with pin arrays attached to hot wall. Applied Thermal Engineering. 2011 Nov 30;31(16):3189-95.

[36] Taguchi G, Elsayed EA, Hsiang TC. Quality engineering in production systems. New York: McGraw-Hill; 1989 Jan.

[37] Alinejad J, Esfahani JA. Taguchi design of three dimensional simulations for optimization of turbulent mixed convection in a cavity. Meccanica. 2017Mar1;52(4-5):925-38.